

Thermal decomposition of SO_4^{2-} -intercalated Mg–Al layered double hydroxide

Elimination behavior of sulfur oxides

Tomohito Kameda · Yuki Fubasami ·
Toshiaki Yoshioka

Received: 21 June 2011 / Accepted: 2 August 2011 / Published online: 21 August 2011
© Akadémiai Kiadó, Budapest, Hungary 2011

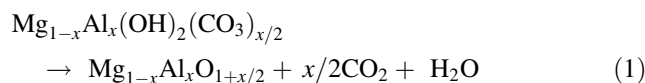
Abstract The thermal properties of SO_4^{2-} -intercalated Mg–Al layered double hydroxide (SO_4 ·Mg–Al LDH) were investigated using simultaneous thermogravimetry–mass spectrometry (TG–MS), and the elimination behavior of sulfur oxides from this double hydroxide was examined. The TG–MS results showed that SO_4 ·Mg–Al LDH decomposed in five stages. The first stage involved evaporation of surface-adsorbed water and interlayer water in SO_4 ·Mg–Al LDH. In the second, third, and fourth stages, dehydroxylation of the brucite-like octahedral layers in SO_4 ·Mg–Al LDH occurred. The fifth stage corresponded to the elimination of SO_4^{2-} intercalated in the interlayer of Mg–Al LDH, producing SO_2 and SO_3 . The thermal decomposition of SO_4 ·Mg–Al LDH resulted in the formation of SO_2 and SO_3 at 900–1000 °C, which then reacted with H_2O to form H_2SO_3 and H_2SO_4 . The elimination of sulfur oxides increased with the decomposition time and temperature. Almost all of the intercalated SO_4^{2-} was desulfurized from SO_4 ·Mg–Al LDH at 1000 °C; however, Mg–Al oxide was not formed due to the production of MgO and MgAl_2O_4 .

Keywords Elimination · Sulfur oxides · Mg–Al layered double hydroxide · Thermal decomposition · TG–MS

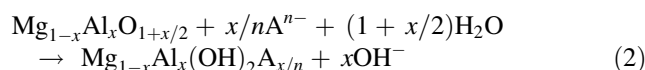
Introduction

Mg–Al layered double hydroxide (Mg–Al LDH) is represented by the formula $[\text{Mg}_{1-x}\text{Al}_x]^{2+}(\text{OH})_2(\text{A}^{n-})_{x/n} \cdot m\text{H}_2\text{O}$,

where A^{n-} is an anion, such as CO_3^{2-} or SO_4^{2-} , and x is the Al/(Mg + Al) molar ratio ($0.20 \leq x \leq 0.33$) [1, 2]. Mg–Al LDH consists of brucite-like octahedral layers that are positively charged due to the replacement of some Mg^{2+} units by Al^{3+} , while the interlayer anions help to maintain the charge balance. Water (H_2O) molecules occupy the remaining spaces in the interlayer. CO_3^{2-} -intercalated Mg–Al LDH (CO_3 ·Mg–Al LDH) can be converted to Mg–Al oxide by calcination at 450–800 °C. The formation of Mg–Al oxide is represented by the following reaction:



The resulting Mg–Al oxide undergoes rehydration and combines with anions to afford the original LDH structure, as shown in the following equation:



Frost's review presents that the thermal decomposition of CO_3 ·Mg–Al LDH, which is the representative LDH, occurs in three steps: (i) removal of adsorbed water, (ii) elimination of the interlayer structural water, and (iii) simultaneous dehydroxylation and decarbonation of the hydrotalcite framework [3]. Mg–Al LDH and Mg–Al oxide can be used as an adsorbent for the removal of anionic pollutants in aqueous solution [4–9]. The abovementioned rehydration and subsequent combination of Mg–Al oxide with anions in solution are accompanied by the release of OH^- . Previously, we have found that Mg–Al oxide is excellent for the treatment of mineral acids, such as H_3PO_4 , H_2SO_4 , HCl , and HNO_3 [10]. That is, Mg–Al oxide can neutralize and fix PO_4^{3-} , SO_4^{2-} , Cl^- , and NO_3^- in the interlayer of reconstructed Mg–Al LDH.

T. Kameda (✉) · Y. Fubasami · T. Yoshioka
Graduate School of Environmental Studies, Tohoku University,
6-6-07 Aoba, Aramaki, Aoba-ku, Sendai 980-8579, Japan
e-mail: kameda@env.che.tohoku.ac.jp

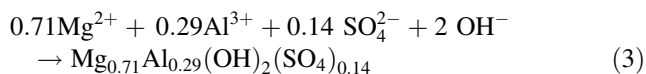
Treatment of HCl with Mg–Al oxide results in the reconstruction of Cl[−]-intercalated Mg–Al LDH (Cl·Mg–Al LDH). We also found that the thermal decomposition of Cl·Mg–Al LDH produced HCl with the reformation of Mg–Al oxide [11, 12]. The treatment of HNO₃ with Mg–Al oxide results in the reconstruction of NO₃[−]-intercalated Mg–Al LDH (NO₃·Mg–Al LDH). The NO₃·Mg–Al LDH produces NO₂ during its thermal decomposition, which reacts with H₂O and O₂, forming HNO₃ and HNO₂ [13]. The treatment of H₂SO₄ with Mg–Al oxide results in the reconstruction of SO₄^{2−}-intercalated Mg–Al LDH (SO₄·Mg–Al LDH). In practical waste H₂SO₄ treatment, the produced SO₄·Mg–Al LDH must be further treated in order to reduce the solid waste. One of the treatment is the calcination of SO₄·Mg–Al LDH. Therefore, it is necessary to examine in detail the thermal decomposition behavior of SO₄·Mg–Al LDH and the elimination of sulfur oxides.

In this study, we investigated the thermal properties of SO₄·Mg–Al LDH by simultaneous thermogravimetry–mass spectrometry (TG–MS). Additionally, we investigated the thermal decomposition of SO₄·Mg–Al LDH in air to determine the effect of temperature on the elimination behavior of sulfur oxides.

Experimental

Preparation

SO₄·Mg–Al LDH was prepared by the co-precipitation method, as expressed in Eq. 3.



The Mg–Al solution (0.36 M MgSO₄ + 0.14 M Al₂(SO₄)₃) was prepared by dissolving MgSO₄ (0.089 mol) and Al₂(SO₄)₃ (0.018 mol) in 250 mL of deionized water. The Mg–Al solution was added dropwise to 250 mL of 0.14 M

Na₂SO₄ solution at 30 °C with mild agitation. The solution pH was adjusted to 10.5 by adding 0.5 M NaOH solution. The mixture was then stirred continuously at 30 °C for 1 h. The SO₄·Mg–Al LDH formed was isolated by filtration and the resulting suspension was washed thoroughly with deionized water and dried under reduced pressure (133 Pa) at 40 °C for 40 h. The SO₄·Mg–Al LDH crystals were ground into a powder using a mortar and pestle, and then characterized by X-ray diffraction (XRD) using a Rigaku RINT-2200VHF diffractometer (Rigaku Corp., Tokyo, Japan) with Cu K α radiation at 40 kV and 20 mA (scan rate: 2° min^{−1}). The SO₄·Mg–Al LDH was dissolved in 1 M HNO₃, and analyzed for Mg²⁺ and Al³⁺ using inductively coupled plasma–atomic emission spectrometry (ICP–AES). The SO₄·Mg–Al LDH was also dissolved in 0.1 M HCl, and analyzed for SO₄^{2−} using a Dionex DX-120 ion chromatograph equipped with an AS-12A column (eluent: 2.7 mM Na₂CO₃ and 0.3 mM NaHCO₃; flow rate: 1.3 mL min^{−1}).

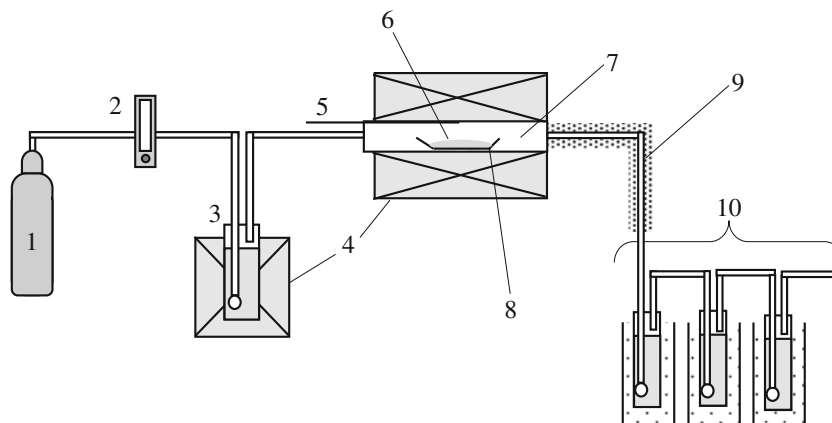
Thermal properties of SO₄·Mg–Al LDH

A 10-mg sample of SO₄·Mg–Al LDH was analyzed by simultaneous TG (Seiko Instruments TG/DTA 6200) and MS (Hewlett Packard 5973) at a heating rate of 5 °C min^{−1} in a He flow rate of 100 mL min^{−1}. The decomposition products were introduced to the MS ion source through an inactivated stainless steel capillary tube heated at 300 °C to prevent condensation of the evolved products.

Elimination behavior of sulfur oxides from SO₄·Mg–Al LDH

The experimental apparatus used to study the thermal decomposition of SO₄·Mg–Al LDH is illustrated in Fig. 1. An aluminum boat containing 0.5 g of SO₄·Mg–Al LDH was inserted in a quartz reaction tube, which was placed in an electric furnace. SO₄·Mg–Al LDH decomposed at 800–1000 °C at an air flow rate of 50 mL min^{−1}. The

Fig. 1 Experimental apparatus used for thermal decomposition of SO₄·Mg–Al LDH. 1 Air cylinder, 2 flow meter, 3 water vapor generator, 4 electric furnace, 5 thermocouple, 6 sample, 7 quartz reaction tube, 8 aluminum boat, 9 flexible heater, 10 water trap (0 °C)



evolved gas was collected in three water traps (0 °C) containing 30 mL of deionized water. To prevent condensation of the evolved gas, the line from the quartz reaction tube to the trap was heated to 110–140 °C using a flexible heater. Anions in the traps were quantified using an ion chromatograph. The products obtained from the thermal decomposition of $\text{SO}_4\cdot\text{Mg-Al}$ LDH were identified by XRD analysis. For the experiment under steam using a water vapor generator, the $\text{SO}_4\cdot\text{Mg-Al}$ LDH was decomposed for 2 h under air flow containing water vapor (partial pressure: 30%) at 50 mL min^{-1} .

Results and discussion

Preparation

The XRD patterns obtained for $\text{SO}_4\cdot\text{Mg-Al}$ LDH (Fig. 2) were ascribed to hydrotalcite (JCPDS card 22-700), a naturally occurring hydroxycarbonate of magnesium and aluminum ($\text{Mg}_6\text{Al}_2(\text{OH})_{16}\text{CO}_3\cdot 4\text{H}_2\text{O}$), and revealed that $\text{SO}_4\cdot\text{Mg-Al}$ LDH has an LDH structure. The basal spacing (d_{003}) of 8.7 Å was similar to that of $\text{SO}_4\cdot\text{Mg-Al}$ LDH (8.6 Å) reported by Sato et al. [14], suggesting the intercalation of SO_4^{2-} in the interlayer of prepared Mg-Al LDH. Table 1 lists the chemical composition of $\text{SO}_4\cdot\text{Mg-Al}$ LDH. The molar ratios of Mg/Al and SO_4/Al were 2.6 and 0.60, respectively. The Mg/Al molar ratio was similar to the expected value for the preparation procedure in this study. The SO_4/Al molar ratio was 120% of the expected value, which was calculated from the neutralization of the positive charge of the Al-bearing brucite-like octahedral layers. This suggests that the SO_4^{2-} content in $\text{SO}_4\cdot\text{Mg-Al}$

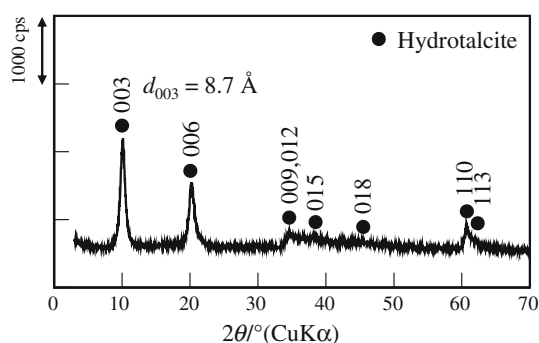


Fig. 2 XRD patterns for $\text{SO}_4\cdot\text{Mg-Al}$ LDH

Table 1 Chemical composition of $\text{SO}_4\cdot\text{Mg-Al}$ LDH

Mass%			Molar ratio	
Mg	Al	SO_4	Mg/Al	SO_4/Al
15.6	6.7	14.2	2.6	0.60

LDH is governed by the charge balance in Mg-Al LDH, and some SO_4^{2-} is adsorbed on the surface of Mg-Al LDH. As a result, SO_4^{2-} -intercalated Mg-Al LDH was confirmed to be prepared by the co-precipitation method.

Thermal properties of $\text{SO}_4\cdot\text{Mg-Al}$ LDH

Figure 3 shows the TG and derivative thermogravimetry (DTG) curves for $\text{SO}_4\cdot\text{Mg-Al}$ LDH. The decomposition of $\text{SO}_4\cdot\text{Mg-Al}$ LDH occurred in the following five stages: (1) mass loss of 0–14% until 210 °C, (2) mass loss of 14–24% at 210–430 °C, (3) mass loss of 24–33% at 430–490 °C, (4) mass loss of 33–38% at 490–800 °C, and (5) mass loss of 38–42% above 800 °C. The first stage corresponded to the evaporation of surface-adsorbed water and interlayer water in $\text{SO}_4\cdot\text{Mg-Al}$ LDH. The second, third, and fourth stages were attributable to the dehydroxylation of the brucite-like octahedral layers in $\text{SO}_4\cdot\text{Mg-Al}$ LDH. The fifth stage was most probably due to the elimination of SO_4^{2-} intercalated in the Mg-Al LDH interlayers. Figure 4 shows the selected-ion mass spectra of major products formed from the thermal decomposition of $\text{SO}_4\cdot\text{Mg-Al}$ LDH. The mass spectrum exhibited signals at m/z 18, 32, and 64, corresponding to the molecular ion peaks of H_2O^+ , O_2^+ , and SO_2^+ , respectively. The H_2O^+ peak in the spectrum indicated that H_2O was produced during the elimination of surface-adsorbed water and interlayer water at stage 1, the dehydroxylation of $\text{SO}_4\cdot\text{Mg-Al}$ LDH components whose properties were similar to those of $\text{Al}(\text{OH})_3$ at stage 2, the dehydroxylation of $\text{SO}_4\cdot\text{Mg-Al}$ LDH components whose properties were similar to those of $\text{Mg}(\text{OH})_2$ at stage 3, and the dehydroxylation of $\text{SO}_4\cdot\text{Mg-Al}$ LDH components whose properties were similar to those of $\text{Al}(\text{OH})_3$ at stage 4. We have already

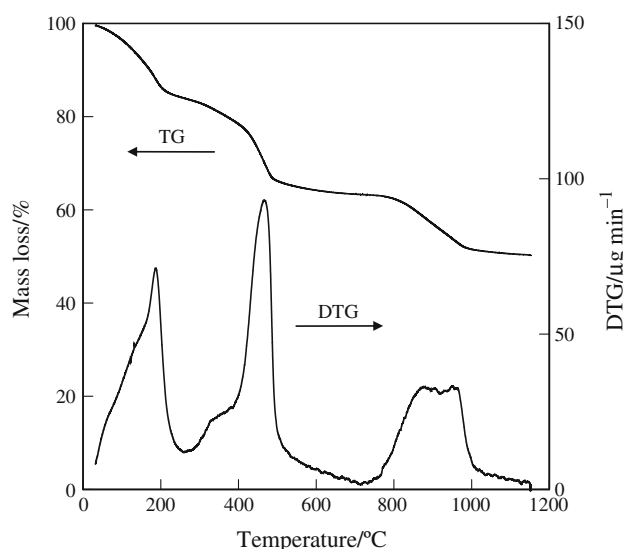


Fig. 3 TG and DTG curves for $\text{SO}_4\cdot\text{Mg-Al}$ LDH

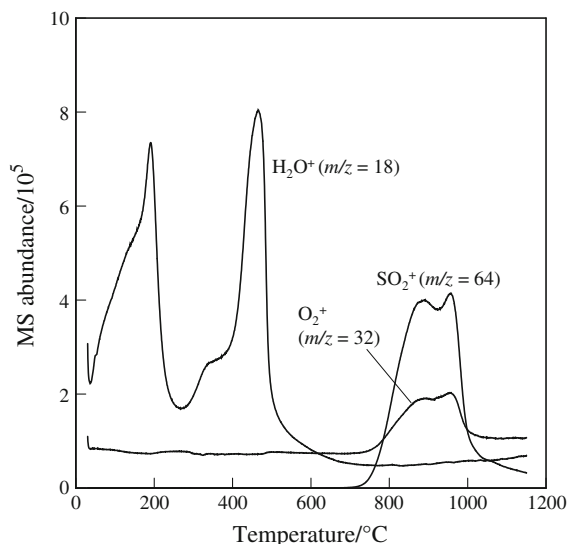


Fig. 4 Selected-ion mass spectra of major products formed in the thermal decomposition of $\text{SO}_4\cdot\text{Mg–Al LDH}$

clarified this division of the dehydroxylation process of Mg–Al LDH into three stages by applying MS spectra of H_2O during the thermal decomposition of $\text{Mg}(\text{OH})_2$ and $\text{Al}(\text{OH})_3$ [11, 13]. The SO_2^+ and O_2^+ peaks were observed over 750°C in the mass spectra, corresponding to the fifth (decomposition) stage in the TG curve. The SO_2^+ peak corresponds to the occurrence of SO_2 and SO_3 . This indicates that the mass loss of $\text{SO}_4\cdot\text{Mg–Al LDH}$ in the fifth stage was due to the formation of SO_2 and SO_3 by the elimination of intercalated SO_4^{2-} . The O_2^+ peak corresponds to the production of O_2 , derived from the decomposition of SO_4^{2-} in $\text{SO}_4\cdot\text{Mg–Al LDH}$ in the fifth stage. The relationships among SO_2 , SO_3 , and O_2 are expressed as follows:



In summary, the decomposition of $\text{SO}_4\cdot\text{Mg–Al LDH}$ proceeded in five stages. Stage 1: evaporation of surface-adsorbed water and interlayer water in $\text{SO}_4\cdot\text{Mg–Al LDH}$. Stages 2, 3, and 4: dehydroxylation of the brucite-like octahedral layers in $\text{SO}_4\cdot\text{Mg–Al LDH}$. Stage 5: elimination of SO_4^{2-} intercalated in the interlayer of Mg–Al LDH to produce SO_2 and SO_3 .

Elimination behavior of sulfur oxides from $\text{SO}_4\cdot\text{Mg–Al LDH}$

We examined the elimination behavior of sulfur oxides from $\text{SO}_4\cdot\text{Mg–Al LDH}$ using the experimental apparatus depicted in Figure 1 and the production of Mg–Al oxide. The temperature range examined was $800\text{--}1000^\circ\text{C}$, corresponding to the fifth stage of the TG curve (Fig. 3).

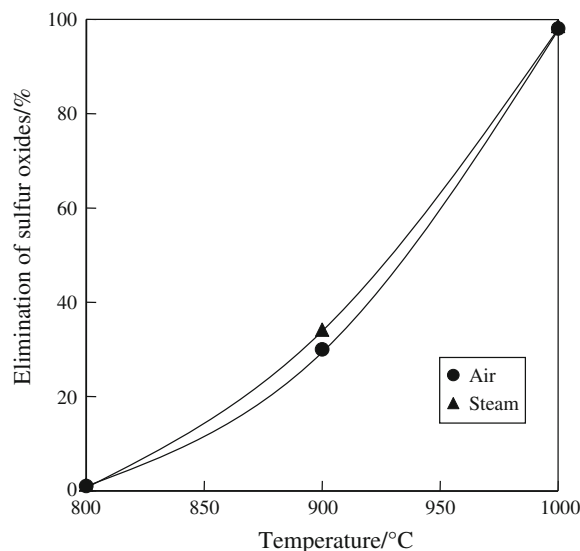
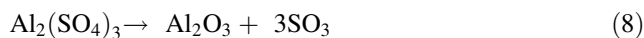


Fig. 5 Effect of temperature and atmosphere on the elimination of sulfur oxides in the thermal decomposition of $\text{SO}_4\cdot\text{Mg–Al LDH}$ for 2 h

Figure 5 shows the effect of temperature and atmosphere on the elimination of sulfur oxides in the thermal decomposition of $\text{SO}_4\cdot\text{Mg–Al LDH}$ for 2 h. Because SO_4^{2-} and SO_3^{2-} were detected in the water traps, the unstable SO_3^{2-} was oxidized by 0.15% H_2O_2 to SO_4^{2-} , followed by quantification using ion chromatography. The elimination of sulfur oxides is expressed as the ratio of the mole percent of SO_4^{2-} in the traps to that of SO_4^{2-} in $\text{SO}_4\cdot\text{Mg–Al LDH}$. In both air and steam, the elimination of sulfur oxides increased with increasing temperature, and was $>98\%$ at 1000°C . The solutions in the traps were acidic, suggesting the production of H_2SO_3 and H_2SO_4 . The thermal decomposition of $\text{SO}_4\cdot\text{Mg–Al LDH}$ resulted in the formation of SO_2 and SO_3 . SO_2 and SO_3 then react with H_2O to form H_2SO_3 and H_2SO_4 , as described in Eqs. 5 and 6, respectively.



In both cases, the thermal decomposition of $\text{SO}_4\cdot\text{Mg–Al LDH}$ at 800°C did not produce sulfur oxides. The elimination of sulfur oxides in steam was similar to that in air at all temperatures. The steam did not promote the desulfurization of $\text{SO}_4\cdot\text{Mg–Al LDH}$, although it did promote the dehydrochlorination of $\text{Cl}\cdot\text{Mg–Al LDH}$ [11]. This is related to the fact that the desulfurization of $\text{SO}_4\cdot\text{Mg–Al LDH}$ does not require H_2O . The thermal properties of sulfates on $\text{SO}_4\cdot\text{Mg–Al LDH}$ are assumed to resemble those of MgSO_4 and $\text{Al}_2(\text{SO}_4)_3$. The desulfurization of MgSO_4 and $\text{Al}_2(\text{SO}_4)_3$ is expressed as follows:



These reactions do not require H_2O . Thus, steam did not play a role in the desulfurization of $\text{SO}_4\cdot\text{Mg-Al}$ LDH, in contrast to the case of the dehydrochlorination of $\text{Cl}\cdot\text{Mg-Al}$ LDH. Figure 6 shows the variation in the elimination of sulfur oxides with time in the thermal decomposition of $\text{SO}_4\cdot\text{Mg-Al}$ LDH at $1000\text{ }^\circ\text{C}$ in air. The elimination of sulfur oxides increased gradually from 0 to 30 min, increased rapidly from 30 to 60 min, reaching about 95% at 60 min, and increased slightly from 60 to 180 min. Almost all of the intercalated SO_4^{2-} was lost from $\text{SO}_4\cdot\text{Mg-Al}$ LDH at $1000\text{ }^\circ\text{C}$, which explains why the SO_2^+ peak was detected primarily in the mass spectrum until $1000\text{ }^\circ\text{C}$ (Fig. 4). Figure 7 shows the XRD patterns for the products obtained from the thermal decomposition of $\text{SO}_4\cdot\text{Mg-Al}$ LDH under different heating conditions. Although Mg-Al oxide was obtained at $800\text{ }^\circ\text{C}$ after 120 min, XRD peaks ascribed to MgSO_4 and $\text{MgSO}_4\cdot 6\text{H}_2\text{O}$ were also observed. These observations are in good agreement with the results reported by Miyata and Okada [15]. The production of MgSO_4 and $\text{MgSO}_4\cdot 6\text{H}_2\text{O}$ supports that the elimination of sulfur oxides at $800\text{ }^\circ\text{C}$ was around 1% (Fig. 5). The product at $900\text{ }^\circ\text{C}$ after 120 min was a mixture of MgO , MgAl_2O_4 , MgSO_4 , and $\text{MgSO}_4\cdot 6\text{H}_2\text{O}$. The production of MgO and MgAl_2O_4 is attributed to the decomposition of Mg-Al oxide. At $1000\text{ }^\circ\text{C}$ after 180 min, crystal growth of MgO and MgAl_2O_4 was observed, and the XRD peaks ascribed to MgSO_4 and $\text{MgSO}_4\cdot 6\text{H}_2\text{O}$ disappeared, confirming the desulfurization of $\text{SO}_4\cdot\text{Mg-Al}$ LDH. In contrast with the case of $\text{Cl}\cdot\text{Mg-Al}$ LDH and $\text{NO}_3\cdot\text{Mg-Al}$ LDH [12, 13], the thermal decomposition of $\text{SO}_4\cdot\text{Mg-Al}$ LDH did not result in the formation of Mg-Al oxide alone.

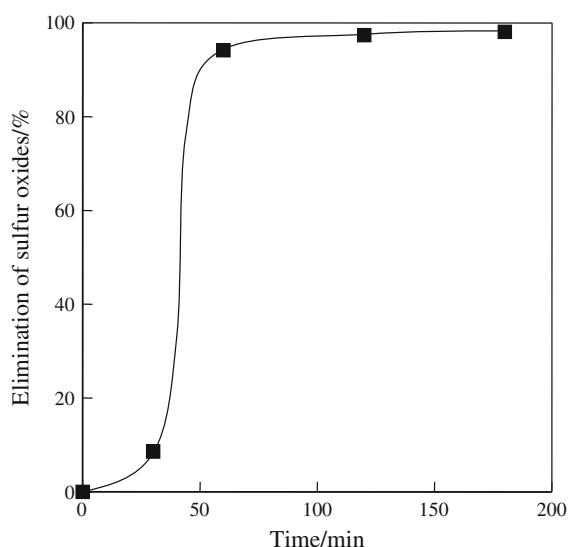


Fig. 6 Variation in the elimination of sulfur oxides over time from the thermal decomposition of $\text{SO}_4\cdot\text{Mg-Al}$ LDH at $1000\text{ }^\circ\text{C}$ in air

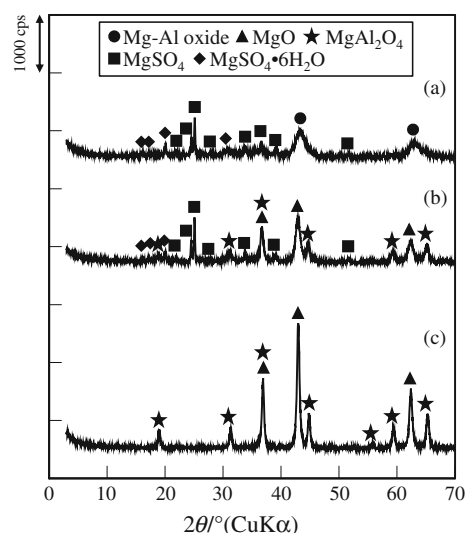


Fig. 7 XRD patterns for products obtained from the thermal decomposition of $\text{SO}_4\cdot\text{Mg-Al}$ LDH under different heating conditions: (a) $800\text{ }^\circ\text{C}$, 120 min; (b) $900\text{ }^\circ\text{C}$, 120 min; (c) $1000\text{ }^\circ\text{C}$, 180 min

Taken together, the thermal decomposition of $\text{SO}_4\cdot\text{Mg-Al}$ LDH at $800\text{ }^\circ\text{C}$ could not produce sulfur oxides, although Mg-Al oxide was obtained with by-products. On the other hand, the thermal decomposition of $\text{SO}_4\cdot\text{Mg-Al}$ LDH at $1000\text{ }^\circ\text{C}$ could not form Mg-Al oxide; however, almost all of the intercalated SO_4^{2-} was desulfurized from $\text{SO}_4\cdot\text{Mg-Al}$ LDH.

Conclusions

In summary, the thermal decomposition of $\text{SO}_4\cdot\text{Mg-Al}$ LDH occurred in the following five stages: evaporation of surface-adsorbed water and interlayer water (stage 1), dehydroxylation of the brucite-like octahedral layers in $\text{SO}_4\cdot\text{Mg-Al}$ LDH (stages 2, 3, and 4), and elimination of SO_4^{2-} intercalated in the interlayer of Mg-Al LDH to produce SO_2 and SO_3 (stage 5). The thermal decomposition of $\text{SO}_4\cdot\text{Mg-Al}$ LDH resulted in the formation of SO_2 and SO_3 at $900\text{--}1000\text{ }^\circ\text{C}$, which then reacted with H_2O to form H_2SO_3 and H_2SO_4 . The elimination of sulfur oxides increased with decomposition time and temperature. Almost all of the intercalated SO_4^{2-} was desulfurized from $\text{SO}_4\cdot\text{Mg-Al}$ LDH at $1000\text{ }^\circ\text{C}$; however, Mg-Al oxide was not formed, due to the production of MgO and MgAl_2O_4 .

The treatment of H_2SO_4 with Mg-Al oxide results in the production of $\text{SO}_4\cdot\text{Mg-Al}$ LDH. The calcination of $\text{SO}_4\cdot\text{Mg-Al}$ LDH could yield H_2SO_4 , making it available for practical use. The decomposition products, MgO and MgAl_2O_4 , are considered to be useful as refractory materials, leading to the reduction of the solid waste.

References

1. Ingram L, Taylor HFW. The crystal structures of sjogrenite and pyroaurite. *Mineral Mag.* 1967;36:465–79.
2. Allmann R. The crystal structure of pyroaurite. *Acta Cryst.* 1968; B24:972–7.
3. Palmer SJ, Frost RL, Nguyen T. Hydrotalcites and their role in coordination of anions in Bayer liquors: anion binding in layered double hydroxides. *Coord Chem Rev.* 2009;253:250–67.
4. Auxilio AR, Andrews PC, Junk PC, Spiccia L, Neumann D, Raverty W, Vanderhoek N. Adsorption and intercalation of Acid Blue 9 on Mg–Al layered double hydroxides of variable metal composition. *Polyhedron.* 2007;26:3479–90.
5. Cornejo J, Celis R, Pavlovic I, Ulibarri MA. Interactions of pesticides with clays and layered double hydroxides: a review. *Clay Miner.* 2008;43:155–75.
6. Wang SL, Liu CH, Wang MK, Chuang YH, Chiang PN. Arsenate adsorption by Mg/Al–NO₃ layered double hydroxides with varying the Mg/Al ratio. *Appl Clay Sci.* 2009;43:79–85.
7. Wu Y, Chi Y, Bai H, Qian G, Cao Y, Zhou J, Xu Y, Liu Q, Xu ZP, Qiao S. Effective removal of selenate from aqueous solutions by the Friedel phase. *J Hazard Mater.* 2010;176:193–8.
8. Douglas GB, Wendling LA, Pleysier R, Trefry MG. Hydrotalcite formation for contaminant removal from ranger mine process water. *Mine Water Environ.* 2010;29:108–15.
9. Wajima T, Shimizu T, Yamato T, Ikegami Y. Removal of NaCl from seawater using natural zeolite. *Toxicol Environ Chem.* 2010;92:21–6.
10. Kameda T, Yabuuchi F, Yoshioka T, Uchida M, Okuwaki A. New method of treating dilute mineral acids using magnesium–aluminum oxide. *Water Res.* 2003;37:1545–50.
11. Kameda T, Yoshioka T, Watanabe K, Uchida M, Okuwaki A. Dehydrochlorination behavior of a chloride ion–intercalated hydrotalcite-like compound during thermal decomposition. *Appl Clay Sci.* 2007;35:173–9.
12. Kameda T, Yoshioka T, Watanabe K, Uchida M, Okuwaki A. Dehydrochlorination and recovery of hydrochloric acid by thermal treatment of a chloride ion–intercalated hydrotalcite-like compound. *Appl Clay Sci.* 2007;37:215–9.
13. Kameda T, Fubasami Y, Uchiyama N, Yoshioka T. Elimination behavior of nitrogen oxides from a NO₃[−]-intercalated Mg–Al layered double hydroxide during thermal decomposition. *Thermochim Acta.* 2010;499:106–10.
14. Sato T, Wakabayashi T, Shimada M. Adsorption of various anions by magnesium aluminum oxide (Mg_{0.7}Al_{0.3}O_{1.15}). *Ind Eng Chem Prod Res Dev.* 1986;25:89–92.
15. Miyata S, Okada A. Synthesis of hydrotalcite-like compounds and their physico-chemical properties-The systems Mg²⁺–Al³⁺–SO₄^{2−} and Mg²⁺–Al³⁺–CrO₄^{2−}. *Clays Clay Miner.* 1977;25:14–8.